Galvanomagnetic properties and band structure of monoclinic $SrAs_3$

P. J. Klar and W. Bauhofer
Technische Universität Hamburg-Harburg, Materialien der Mikroelektronik, D-21071 Hamburg, Federal Republic of Germany
(Received 11 January 1994)

The unusual galvanomagnetic properties of the monoclinic semimetal $SrAs_3$, first-order longitudinal Hall effect and magnetoresistivity in Hall geometry, are quantitatively described within a two-band model. The ten model parameters for $T \rightarrow 0$ K are obtained from a fit to 14 low-field coefficients in combination with high-field Hall data and Shubnikov–de Haas oscillations. The temperature variation of the galvanomagnetic coefficient can be explained most convincingly with three temperature-dependent parameters, i.e., electron and hole scattering times and electron concentration, while the anisotropy ratios are kept constant. An energy gap of 38 meV for the temperature activation of the electrons is derived from this procedure.

I. INTRODUCTION

A first-order longitudinal Hall effect (LHE) has recently been observed for the monoclinic compounds $SrAs_3$,[1] $CaAs_3$, and $AuTe_2$.[2] The geometrical arrangement for a LHE is characterized by a magnetic field parallel either to the current or the Hall field. In principle, such unusual galvanomagnetic coefficients may exist in low-symmetry crystals. It has been found, however, that the occurrence of significant LHE coefficients is restricted to temperature ranges representing two-band regimes.[2] $SrAs_3$ represents an ideal material for such investigations since its conduction type changes from two-band behavior at low temperatures to predominantly n type at 300 K due to an increase of the electron density. The accompanying decrease of the mobilities leads to a small residual resistance ratio $\rho(300\ \mathrm{K})/\rho(4\ \mathrm{K})$ of about 4. The experimental observations have been interpreted in the following way: A single band with monoclinic symmetry cannot produce a significant LHE. A necessary prerequisite is the existence of two quasiellipsoidal bands whose principal axes are rotated with respect to each other.

The above interpretation of the microscopic origin of the LHE has been verified in a recent theoretical investigation,[3] where different model band structures were used to calculate the resistivity and Hall coefficients of $SrAs_3$ in the limit $T \rightarrow 0$ K. It was shown that a single-band model based on a realistic Fermi surface with monoclinic symmetry cannot reproduce the magnitude of the experimentally observed low-temperature values for the LHE coefficients. However, a quantitative description of the measured LHE can be obtained on the basis of an ellipsoidal two-band model. In this case, the electron and hole concentrations were derived from earlier Shubnikov–de Haas (SdH) data performed on a different batch of samples.[4] The remaining eight mobility parameters (four for each band) are exactly fitted to the eight measured resistivity (three) and Hall (five) coefficients. As has already been noted in Ref. 3, the parameters deduced for the electron band contain two severe inconsistencies. The first problem is concerned with the determination of the electron concentration. In a first approximation, this number was derived from a weak SdH oscillation,[4] assuming a spherical Fermi surface. This assumption is in clear contrast to the extreme anisotropy obtained from the calculation. The other inconsistency is related to the conductivity anisotropy in the ab plane. The fit result of a 3:1 ratio for the $T \rightarrow 0$ K electron conductivities of Ref. 3 (Table IV) is incompatible with the experimentally determined 1:4.5 conductivity ratio at 300 K where electronic conduction is dominant.

In this paper we report on further experimental investigations of the galvanomagnetic properties of $SrAs_3$ to solve the above-mentioned problems. We have measured several magnetoresistivity (MR) components in order to obtain an overdetermined nonlinear system for our fitting procedure. Reliable numbers for the carrier concentrations have been obtained by reexamining the size of the hole Fermi surface in addition to the high-field limit of the Hall coefficients (which gives p-n) on the *same* set of samples as investigated in Ref. 1. We find values differing from those used for the calculations in Ref. 3. The difficulties with the determination of the signs of the LHE coefficients have been outlined earlier.[1] Our recent calculations gave some indications that the LHE components ρ_{131} and ρ_{232} should differ in signs contrary to the values given in Ref. 1. We have again carefully checked these signs and we indeed find that ρ_{131} is negative while ρ_{232} has been confirmed to be positive.

The components of the MR tensor which have been calculated for monoclinic symmetry are discussed in Sec. II. The voluminous expressions are listed in the Appendix. Section III summarizes the additional experimental results. We present SdH measurements, high-field Hall data, and an experimental method for the exact determination of MR coefficients in Hall geometry.

In Sec. IV, we describe the two-band fit for $T \rightarrow 0$ K. We use 14 low-field coefficients together with information about the carrier concentrations from the high-field measurements. The fit gives a satisfactory agreement with the measured values. In particular, the anisotropies for the hole and the electron band reproduce very well the hole effective mass values from the temperature-

dependent SdH data and the (electron) conductivity anisotropy at 300 K. The remarkable success of the fit for $T \to 0$ K gave us the confidence to model the temperature variations of the galvanomagnetic coefficients using a minimum number of temperature-dependent parameters. Thus we keep all anisotropies and the hole concentration at the $T=0$ K values. The temperature dependencies of the measured resistivity and Hall coefficients can be displayed semiquantitatively by fitting isotropic, energy-independent hole and electron relaxation times and the electron concentration. The remaining deviations between experimental and theoretical results are discussed in Sec. VI.

II. TWO-BAND MODEL FOR MONOCLINIC SYMMETRY

The simplest version of a two-band model for monoclinic symmetry based on the assumption of energy-independent relaxation times has been outlined in Ref. 1. Within this model LHE coefficients are obtained as a consequence of the existence of nondiagonal mobility tensor elements. $SrAs_3$ crystallizes in the space group $C2/m$. In the notation of the second setting, b is the twofold axis and the monoclinic angle β is situated between the axes a and c. Following the usual nomenclature[5] the orthogonal laboratory system x_1, x_2, x_3 is adjusted with x_2 parallel to a and x_3 parallel to b. The mobility tensor $\underline{\mu}$ is then expressed by

$$\underline{\mu}=\begin{bmatrix}\mu_{11} & \mu_{12} & 0\\ \mu_{12} & \mu_{22} & 0\\ 0 & 0 & \mu_{33}\end{bmatrix} . \tag{1}$$

The relation between current density $\mathbf{j}$ and electric field $\mathbf{E}$ in the presence of an external magnetic field $\mathbf{B}$ is given for a single band by the Drude approximation

$$\mathbf{j}=qn\mathbf{v}=qn[\underline{\mu}(\mathbf{E}+\mathbf{v}\times\mathbf{B})] . \tag{2}$$

Solving this equation for an arbitrary direction of $\mathbf{B}$ gives

$$\mathbf{j}=\underline{\sigma}(\mathbf{B})\mathbf{E} , \tag{3}$$

with

$$\underline{\sigma}=\frac{en}{N}\begin{bmatrix}\mu_{33}\mu B_1^2+\mu_{11} & \mu_{33}\mu B_1B_2+\mu B_3+\mu_{12} & \mu_{33}\mu B_1B_3-\mu_{33}\mu_{11}B_2+\mu_{12}\mu_{33}B_1\\ \mu_{33}\mu B_1B_2-\mu B_3+\mu_{12} & \mu_{33}\mu B_2^2+\mu_{22} & \mu_{33}\mu B_2B_3+\mu_{22}\mu_{33}B_1-\mu_{12}\mu_{33}B_2\\ \mu_{33}\mu B_1B_3+\mu_{33}\mu_{11}B_2-\mu_{12}\mu_{33}B_1 & \mu_{33}\mu B_2B_3-\mu_{22}\mu_{33}B_1+\mu_{12}\mu_{33}B_2 & \mu_{33}\mu B_3^2+\mu_{33}\end{bmatrix} \tag{4}$$

where the abbreviations

$$\mu=\mu_{11}\mu_{22}-\mu_{12}^2 \tag{5}$$

and

$$N=1+\mu_{11}\mu_{33}B_2^2+\mu_{22}\mu_{33}B_1^2+\mu B_3^2-2\mu_{12}\mu_{33}B_1B_2 \tag{6}$$

have been used.

For the case of the existence of two bands, the individual contributions of holes and electrons have to be added:

$$\mathbf{j}_{\text{tot}}=\mathbf{j}_h+\mathbf{j}_e=(\underline{\sigma}^{(h)}+\underline{\sigma}^{(e)})\mathbf{E} =\underline{\sigma}_{\text{tot}}\mathbf{E} . \tag{7}$$

The tensor of the total specific resistivity $\underline{\rho}_{\text{tot}}$ follows through inversion of $\underline{\sigma}_{\text{tot}}$. The tensor elements $\rho_{ij}(\mathbf{B})$ contain polynomials in B_1, B_2, and B_3 up to order 11 in the numerator and up to order 10 in the denominator. The low-field galvanomagnetic coefficients are now obtained from the expansion

$$\rho_{ij}(\mathbf{B})=\rho_{ij}+\rho_{ijk}B_k+\rho_{ijkl}B_kB_l+O(3) . \tag{8}$$

The Hall coefficients are simply determined from the first-order terms of the numerator by setting all $B_i=0$ in the denominator. The calculation is more complicated for the MR tensor elements. First, the even terms in B up to order 2 are retained. Then the respective coefficients for the zero-field resistivity are substracted. Finally, all B_i are set to zero in the common denominator, and the magnetoresistivities are given by the coefficients of the second-order terms in the numerator.

The two-band expressions for the five independent Hall coefficients and for selected MR tensor elements are presented in the Appendix. All results have been carefully checked by applying symmetry considerations (interchanging the indices 1 and 2, interchanging band types) and by examination of the one- and isotropic two-band limits.

Within the framework of our model the LHE coefficients in monoclinic symmetry are explained by the existence of nondiagonal mobility components.[1] Considering the MR tensor the same argument holds for all symmetry-allowed coefficients ρ_{ijkl} with $i \neq j$ and $k \neq l$ and $\{i,j\} \neq \{k,l\}$ (MR coefficients like ρ_{1212} are allowed even in cubic symmetry). The two-band model produces two special relations in addition to the conditions following from symmetry. In particular, the longitudinal MR component ρ_{3333} turns out to be zero, while the existence of ρ_{1111} and ρ_{2222} relies on the nondiagonal mobility. The other special relation is given by identities equivalent to $\rho_{2331}=\rho_{1332}$.

III. EXPERIMENTAL RESULTS

We have reexamined and supplemented our earlier measurements on $SrAs_3$ (Refs. 1 and 4) by the following investigations: (i) verification of the signs of the LHE

coefficients; (ii) high-field limit of the transverse Hall effect (THE); (iii) measurement of selected magnetoresistivity tensor elements; and (iv) recheck of the size of the Fermi surface from SdH oscillation periods.

A. Hall effect

The determination of the sign of a LHE coefficient yields an additional complication in comparison to THE components whose signs are completely fixed by the direction of two crystallographic axes. The sign of a LHE component depends on the chirality of the crystallographic coordinate system with respect to the laboratory system. The absolute direction of the c axis can be determined using a four-circle x-ray diffractometer. The x-ray beam has to be focused on the edge of the sample because of the strong absorption of the mm-sized single crystals. We found a much simpler method by using the electron channeling mode of a scanning electron microscope. The c-axis orientation can be derived from characteristic electron channeling patterns once the pattern has been identified from preoriented samples. We have investigated the signs of the LHE component on a series of samples oriented with the above-mentioned method. We can confirm our earlier result that ρ_{232} should be positive. For ρ_{131}, however, our earlier assignment has to be revised; ρ_{131} is definitely negative. Thus one of the experimental values used for the fits in Ref. 3 was wrong by 200%.

In the case of closed hole and electron orbitals which should apply for the semimetal $SrAs_3$, the difference $p-n$ of the carrier densities can be obtained from the high-field THE:

$$\rho_{ijk}(B\rightarrow\infty)=\frac{1}{e}/(p-n),(ijk)\in\{(321),(132),(213)\} \; . \tag{9}$$

Figure 1 shows magnetic-field-dependent measurements of the THE coefficients ρ_{321} and ρ_{132}. These coefficients have different signs for $B\rightarrow 0$ T. At high fields, they both converge to the same value of about $+100$ cm^3/C which corresponds to $p-n\approx 6\times 10^{16}$ cm^{-3}. This result clearly indicates that the density values used in Ref. 3 cannot be correct. The structure superimposed on the Hall curves are due to SdH oscillations and will be discussed below in context with the MR data.

B. Magnetoresistivity

For monoclinic symmetry the MR tensor contains 20 independent elements. In practice, not all the elements can be determined experimentally. The MR coefficients ρ_{ijkl} with $i=j=1$ cannot be measured since the easy cleavage plane does not allow for the preparation of samples with the long side parallel to direction 1. A reliable determination of ρ_{ijkl} with $i,j=1,2$ or $k,1=1,2$ is complicated by the fact that an unambiguous substraction of the background is not possible since $\rho_{12}\neq 0$. Finally, for the measurement of ρ_{1313} and ρ_{2323} the necessary rotating sample holder was not available. Thus we are left with eight measurable MR tensor elements in addition to three resistivities and five Hall coefficients.

The coefficient ρ_{2331} represents a MR in "Hall geometry" since it contains a magnetic-field component perpendicular to the voltage-current plane. For the measurement of this coefficient we proceed in the following way. A sample with the current in direction 3 and voltage contacts parallel to direction 2 is rotated around direction 2, with α denoting the angle between the magnetic field and direction 1 [see Fig. 2(a)]. U and I are related by the angle- and field-dependent resistivity $\rho(B,\alpha)$:

$$\begin{aligned}\rho(B,\alpha)&=\rho_{231}B\cos\alpha+\rho_{2331}(B\sin\alpha)(B\cos\alpha)\\&=\rho_{231}B\cos\alpha+\tfrac{1}{2}\rho_{2331}B^2\sin 2\alpha \; .\end{aligned} \tag{10}$$

This measurement geometry offers two advantages. First, the LHE coefficient ρ_{233} for $\alpha=90°$ vanishes and the α scale can be determined exactly from the THE. Second, no further B^2 term is contained in Eq. (10) since ρ_{2311} and ρ_{2333} are identical to zero. However, a small misalignment of the voltage contacts has to be taken into account. This leads to an admixture of contributions parallel to

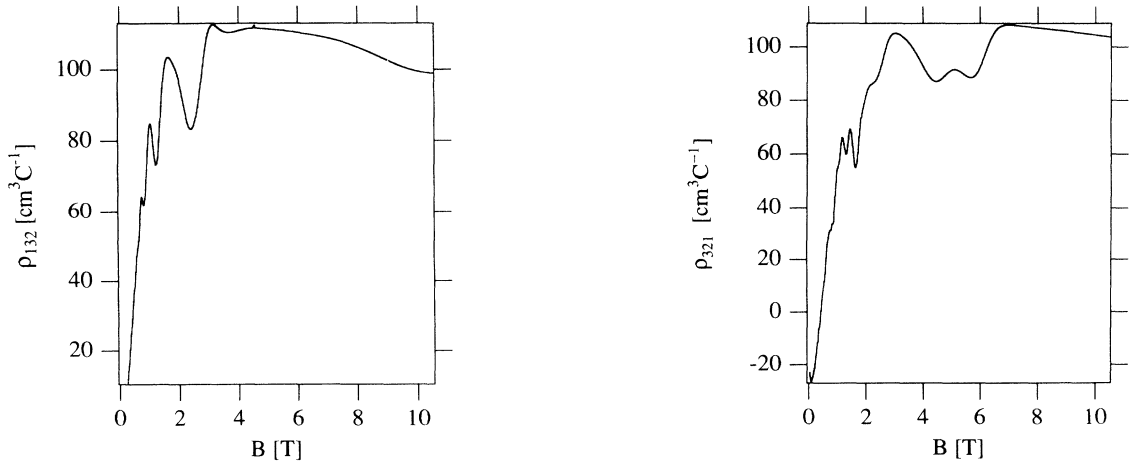

FIG. 1. Magnetic-field dependence of the THE coefficients ρ_{132} (left side) and ρ_{321} (right side) measured at $T=1.5$ K.

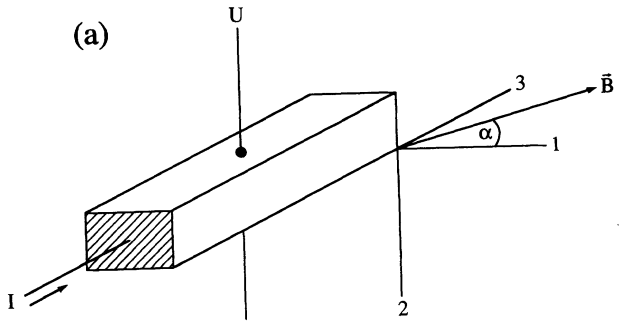

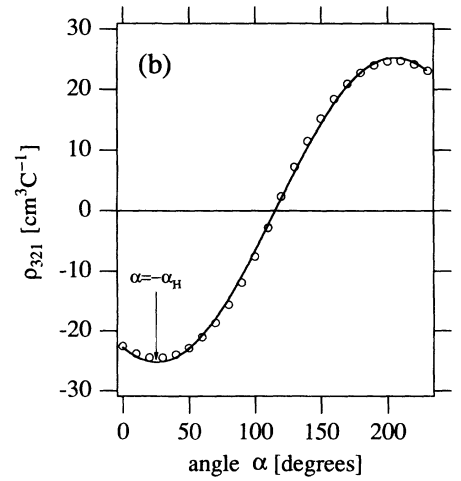

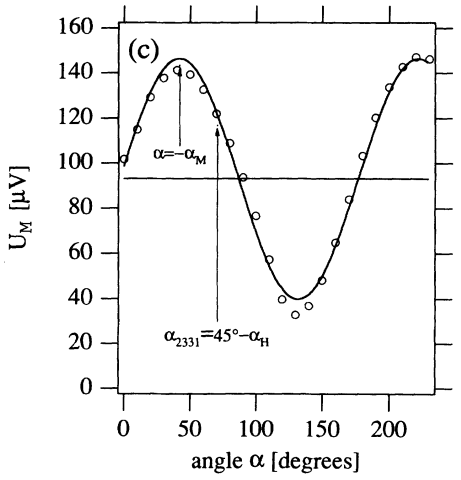

FIG. 2. (a) Geometric arrangement for the measurement of the MR coefficient ρ_{2331}. (b) Angular dependence of ρ_{321} derived from the odd part in B of the voltage U. (c) Even part in B of the voltage U (points). The curve represents a fit according to Eq. (12). ρ_{2331} is evaluated from the oscillatory part of the voltage U_M at α_{2331}.

direction 3. As shown by the measurements, this background can be considerable since it contains the zero-field resistivity ρ_{33} and the normal MR coefficient ρ_{3311}:

$$\rho_{BG}(\alpha)=\rho_{33}+\rho_{3311}B^2\cos^2\alpha+\rho_{3333}B^2\sin^2\alpha$$
$$=\rho_{33}+\tfrac{1}{2}(\rho_{3311}+\rho_{3333})B^2$$
$$+\tfrac{1}{2}(\rho_{3311}-\rho_{3333})B^2\cos^2\alpha\ . \qquad (11)$$

The even part in B of the measured voltage is now fitted by an expression of the form

$$U_M(\alpha)=U_0+U_1\cos[2(\alpha+\alpha_M)]\ . \qquad (12)$$

With $-\alpha_H$ determined from the Hall voltage [odd part in B, Fig. 2(b)], the MR coefficient ρ_{2331} is given by the value of the oscillating part of U_M at the angle $\alpha_{2331}=45°-\alpha_H$ [Fig. 2(c)]. We find a value of

$$\rho_{2331}=-5\times10^4\frac{\mathrm{cm}^5}{CVs}\ , \qquad (13)$$

which cannot, as usual, be normalized by the corresponding zero-field resistivity since $\rho_{23}=0$. To our knowledge, we present here the first measurement of a MR coefficient

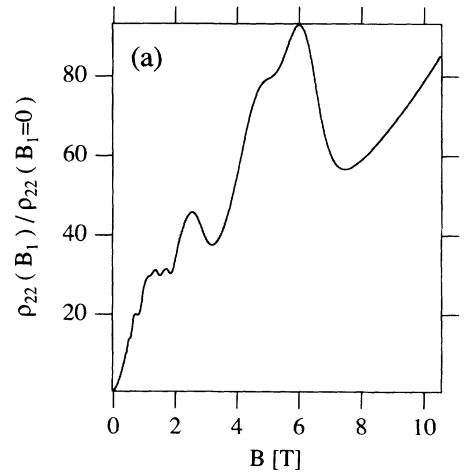

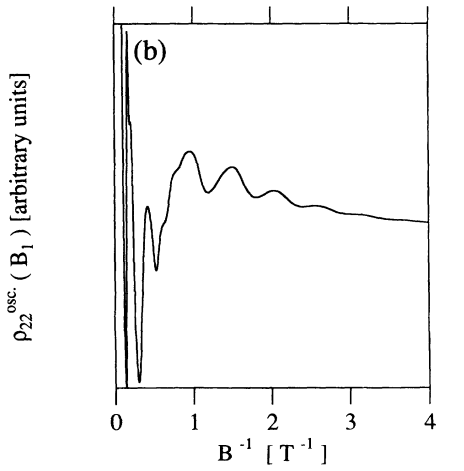

FIG. 3. (a) SdH oscillations of ρ_{22} (B_1) at $T=1.5$ K. (b) Oscillating part of the curve in (a) as a function of $1/B$.

TABLE I. Two-band fit parameter for $T \rightarrow 0$ K.

	$n,p[\mathrm{cm}^{-3}]$	$\mu_{11}\left[\frac{\mathrm{cm}^2}{\mathrm{Vs}}\right]$	$\mu_{22}\left[\frac{\mathrm{cm}^2}{\mathrm{Vs}}\right]$	$\mu_{33}\left[\frac{\mathrm{cm}^2}{\mathrm{Vs}}\right]$	$\mu_{12}\left[\frac{\mathrm{cm}^2}{\mathrm{Vs}}\right]$
holes	1.3×10^{17}	59 700	13 500	256 000	8700
electrons	0.7×10^{17}	−53 000	−108 000	−356 000	50 100

in Hall geometry.

At high magnetic fields the MR coefficients show SdH oscillations as a function of $1/B$. The oscillation period is given by the cross sections of the Fermi bodies perpendicular to the applied field. The size of the Fermi bodies is fixed by the carrier density. Since we had some doubt that the density values determined in Ref. 4 on an early batch of samples with lower mobilities were applicable in the present case, we remeasured the oscillation period for a definite field direction [Fig. 3(a)]. Plotting the oscillating part of ρ_{22} versus $1/B$ [Fig. 3(b)], two different oscillations with periods P of 5 T and about 2 T can be identified. The lower frequency is assigned to the motion of electrons. Then the high-frequency oscillation should be connected with the hole Fermi surface. This value has to be compared with 11.75 T, which has been found in Ref. 4 for the same orientation. Thus the hole density has to be reduced by a factor $(5/11.75)^{3/2}=0.28$. We obtain $p\approx1.9\times10^{17}$ cm^{-3} when again we postulate the existence of two ellipsoidal hole Fermi bodies connected by the twofold axis. Combining the results from SdH and high-field Hall measurements, we use $p\approx1.9\times10^{17}$ cm^{-3} and $p-n=6\times10^{16}$ cm^{-3} as starting values for the two-band fit described in Sec. IV.

IV. MODEL PARAMETERS FOR $T \rightarrow 0$ K

We use 14 low-field galvanomagnetic coefficients (three zero-field resistivities, five Hall coefficients, and six magnetoresistivities) for the determination of ten two-band model parameters. In addition, we fix the difference in densities at $p-n=6\times10^{16}$ cm^{-3}. For the least-squares fit we apply the routine E04UPF which is contained in the NAG Fortran library.[6] The calculations are performed on a Convex 3820.

For the mobilities we use starting values on the order of 10^5 cm^2/V s. Such values are obtained from the approximate relation for the low-field magnetoresistivity:

$$\frac{\Delta\rho}{\rho}\approx(\mu B)^2 . \tag{14}$$

Furthermore, the mobility tensors have to be positive definite. In the course of the calculations we realized that the least-squares routine was not able to move the densities away from their starting values. Therefore, we varied manually the hole density in the range from 1×10^{17} to 2×10^{17} cm^{-3} while keeping the difference $p-n$ constant.

The best fit with a mean deviation of 23% is obtained with the parameters listed in Table I. In Table II, we compare the calculated with the experimental values. The most important result is that the correct sign is found for all Hall coefficients. With two exceptions the experimental values are reproduced by the two-band model within a deviation smaller than 20%. The MR coefficient r_{3322} is underestimated by a factor of 3. The deviation is even larger for the longitudinal MR coefficient r_{2222} which, however, would be zero in an isotropic model. In contrast, the coefficient ρ_{2331} which describes the MR in Hall geometry shows a small difference between calculated and experimental values.

TABLE II. Comparison of experimental galvanomagnetic coefficients with calculated values using the band parameters listed in Table I.

	ρ_{11} [Ω cm]	ρ_{22} [Ω cm]	ρ_{33} [Ω cm]		
experimental	5.22×10^{-4}	5.95×10^{-4}	1.21×10^{-4}		
calculated	5.74×10^{-4}	7.0×10^{-4}	1.08×10^{-4}		
rel. error	0.10	0.18	−0.11		
	$\rho_{132}\left[\frac{\mathrm{cm}^3}{\mathrm{C}}\right]$	$\rho_{213}\left[\frac{\mathrm{cm}^3}{\mathrm{C}}\right]$	$\rho_{321}\left[\frac{\mathrm{cm}^3}{\mathrm{C}}\right]$	$\rho_{131}\left[\frac{\mathrm{cm}^3}{\mathrm{C}}\right]$	$\rho_{232}\left[\frac{\mathrm{cm}^3}{\mathrm{C}}\right]$
experimental	12.3	−9.2	−29.0	−11.6	17.4
calculated	10.5	−8.1	−23.2	−9.5	20.2
rel. error	−0.15	−0.12	−0.20	−0.18	0.16

	$r_{3311}\left[\frac{\mathrm{cm}^4}{\mathrm{V}^2\mathrm{s}^2}\right]$	$r_{3322}\left[\frac{\mathrm{cm}^4}{\mathrm{V}^2\mathrm{s}^2}\right]$	$r_{2211}\left[\frac{\mathrm{cm}^4}{\mathrm{V}^2\mathrm{s}^2}\right]$	$r_{2233}\left[\frac{\mathrm{cm}^4}{\mathrm{V}^2\mathrm{s}^2}\right]$	$r_{2222}\left[\frac{\mathrm{cm}^4}{\mathrm{V}^2\mathrm{s}^2}\right]$	$r_{2331}\left[\frac{\mathrm{cm}^5}{\mathrm{CVs}}\right]$
experimental	8.15×10^9	3.45×10^{10}	1.74×10^{10}	1.99×10^9	8×10^9	-5×10^4
calculated	7.74×10^9	1.07×10^{10}	2.05×10^{10}	2.23×10^9	0.6×10^9	-4.95×10^4
rel. error	−0.05	−0.69	0.18	0.12	−0.93	−0.01

The parameters for electrons and holes obtained from the two-band fit for $T \rightarrow 0$ K can be checked individually by examining whether they are consistent with other experimental results. The assumption of isotropic relaxation times implies a linear relationship between mobility and inverse mass tensor:

$$\underline{\mu} = q\tau \underline{m}^{-1} . \tag{15}$$

Hole effective masses have been determined earlier from the temperature dependence of the amplitudes of SdH oscillations.[4] There, the ratios

$$\frac{m_a^*}{m_b^*} = 20 \quad \text{and} \quad \frac{m_{c^*}^*}{m_b^*} = 6.3 \tag{16}$$

have been found. These values agree well with the corresponding mobility ratios

$$\frac{\mu_{33}^{(h)}}{\mu_{22}^{(h)}} = 19 \quad \text{and} \quad \frac{\mu_{33}^{(h)}}{\mu_{11}^{(h)}} = 4.3 . \tag{17}$$

The hole relaxation time $\tau^{(h)}$ as given by

$$\tau^{(h)} = \frac{\mu_{33}^{(h)} m_b^*}{e} \tag{18}$$

amounts to $\tau^{(h)} = 3.6 \times 10^{-12}$ s, where we have used $m_b^* = 0.0245 m_0$ from Ref. 4.

The electron band parameters can be tested with the resistivity anisotropy at room temperature. At 300 K, the three THE coefficients have a nearly identical value of -1.1 cm^3/C, which is indicative of a predominant electron conduction. Assuming a temperature-independent anisotropy, the 300-K resistivity anisotropy $\rho_{22}/\rho_{33} \approx 4.5$ should be produced from $\mu_{33}^{(e)}/\mu_{22}^{(e)}$ which amounts to 3.3. This is more convincing evidence of the applicability of the two-band model.

The existence of nondiagonal mobility tensor elements μ_{12} corresponds to hole and electron ellipsoids whose principal axes are rotated with respect to the laboratory system in the ac plane. The rotation angle φ is obtained from the relation

$$2\varphi = \arctan \frac{2\mu_{12}}{\mu_{11} - \mu_{22}} . \tag{19}$$

Figure 4 shows the relative positions of the elliptic cross sections in the ac plane. The absolute sizes are not in scale.

Equation (15) and the assumption of ellipsoidal Fermi bodies leads by simple geometrical considerations to a relation between the volume of the Fermi bodies and their cross section in the a^*b^* plane:

$$V = \frac{4\pi}{3} \frac{\mu_{33}}{\sqrt{\mu_{22}\mu_{11}}} \left[\frac{S_{a^*b^*}}{\pi} \right]^{3/2} \left[\frac{\mu_{22} + \mu_{11}\tan^2\theta}{\mu_{33}(1+\tan^2\theta)} \right]^{3/4} , \tag{20}$$

where $\theta = (\pi/2) - \varphi$. Using $n = 2[2/(2\pi)^3]V$ and $S_{a^*b^*} = 2\pi e/\hbar P$ we can carry out a further cross check by calculating the carrier densities from the experimentally determined periods and the fitted mobility tensor components. We obtain $p = 1.3 \times 10^{17}$ cm^{-3} and $n = 0.5 \times 10^{17}$ cm^{-3}, in good agreement with the values given in Table I.

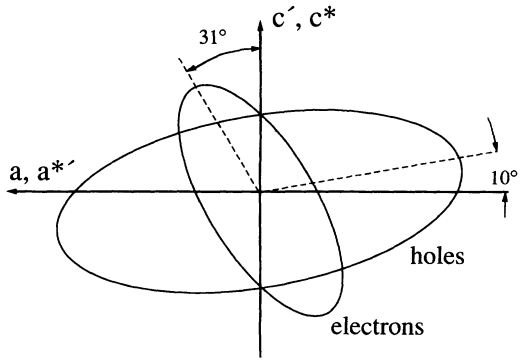

FIG. 4. Cross sections of the electron and hole ellipsoids in the ac plane to illustrate the relative orientations. The ellipses are not in absolute scale.

V. TEMPERATURE DEPENDENCE OF THE BAND PARAMETERS

Starting out from the $T \rightarrow 0$ K fit results, we try to model the temperature dependence of the band parameters based on the assumption of isotropic relaxation times $\tau^{(e)}$ and $\tau^{(h)}$. Neglecting second-order effects this means that the mobility anisotropies and are due to corresponding anisotropies of effective masses and, thereby, do not change with temperature. As a further approximation the hole concentration is fixed at the low temperature value of 1.3×10^{17} cm^{-3}. The remaining three temperature-dependent parameters are fitted to 12 galvanomagnetic coefficients up to 70 K. For $T > 70$ K, we use only resistivities and Hall coefficients since the MR becomes too small to be measured accurately. The fit results are summarized in Fig. 5. The variation of the galvanomagnetic properties of $SrAs_3$ with rising tempera-

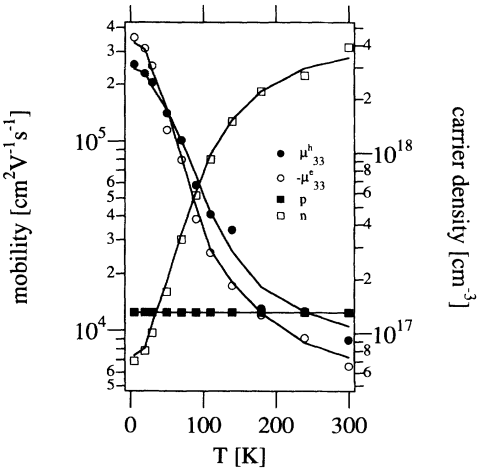

FIG. 5. Temperature variation of hole and electron mobilities, and of the electron density as obtained by fitting the temperature-dependent galvanomagnetic coefficients. The hole density p is fixed at the low-temperature value.

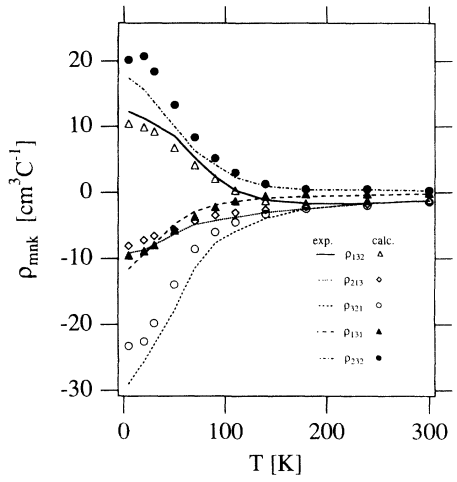

FIG. 6. Comparison of calculated (symbols) and measured (lines) Hall coefficients as a function of temperature.

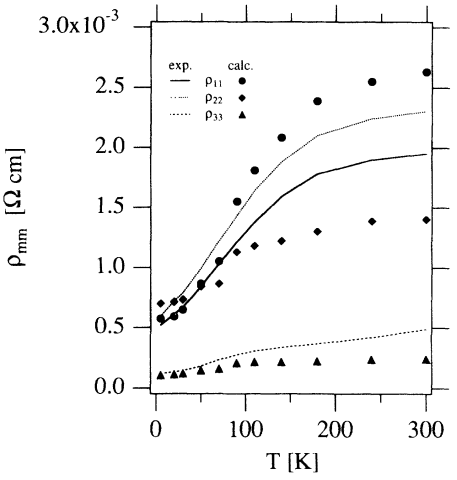

FIG. 7. Comparison of calculated (symbols) and measured (lines) zero-field resistivities as a function of temperature.

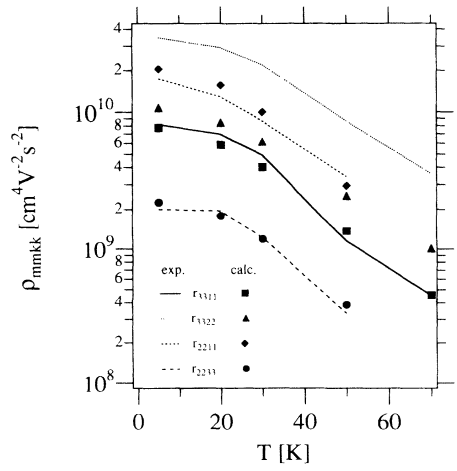

FIG. 8. Comparison of calculated (symbols) and measured (lines) MR coefficients as a function of temperature.

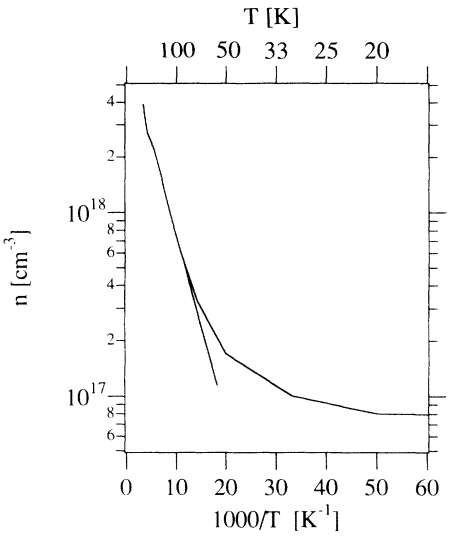

FIG. 9. Logarithm of the calculated electron density as a function of $1000/T$. The slope for $T > 80$ K corresponds to an energy gap of 38 meV.

ture is caused by a decrease of the hole and electron mobility by a factor of 40, and by an increase of the electron concentration factor of 50, between 0 and 300 K. The temperature dependencies of electron and hole mobilities turn out to be qualitatively similar. Assuming the same temperature variation for both bands would not worsen the fit significantly. Thus the description of the temperature-dependent galvanomagnetic properties of $SrAs_3$ can be achieved in our two-band model with a minimum number of independent temperature-varying parameters.

Figures 6–8 clearly show that the measured temperature dependencies are remarkably well reproduced by our simple model. In particular, the sign change of ρ_{132} at 115 K and the vanishing of the LHE coefficients for $T > 150$ K are described quantitatively. The increase of the electron concentration with rising T may be due to a temperature activation across an energy gap. Plotting $\ln n$ versus $1/T$ (see Fig. 9) leads to an energy gap of 38 meV via the relation $n \sim \exp(-E_g/2kT)$. The electrons must stem from a heavy-hole band whose contribution to the conductivity is not significant. In summary, the temperature dependence of the electrical properties of $SrAs_3$ seem to be caused by an intrinsic high mobility hole band, and by highly mobile electrons which are temperature activated from a heavy-hole band across an energy gap of 38 meV.

VI. CONCLUSIONS

We have shown that a significant LHE as observed for the monoclinic semimetal $SrAs_3$ can be explained quantitatively within a simple two-band model. The model parameters for $T \to 0$ K which were obtained by fitting 14 galvanomagnetic coefficients are consistent with an earlier determination of the hole mass anisotropies. The temperature variation of the galvanomagnetic coefficients, in particular the Hall coefficients, can suc-

cessfully be modeled with three temperature-dependent parameters. We do not believe that the remaining deviation between experimental and calculated values can be reduced within the framework of a Drude-type model. Energy-dependent relaxation times and nonellipsoidal Fermi bodies could improve the theoretical results.

The main result of our present work is the conclusive evidence that the LHE in $SrAs_3$ is indeed produced by two bands with differently inclined ellipsoids. We conclude from the equivalence of the experimental results that the same arguments can be used for $CaAs_3$ and $AuTe_2$.

ACKNOWLEDGMENTS

We acknowledge stimulating discussions with Professor R. v. Baltz. We thank Helmut Wendel and Annette Zechmeister for sample preparation.

APPENDIX

The two-band expressions for the zero-field resistivities, the Hall coefficients, and selected MR coefficients are given for monoclinic symmetry. We have omitted all MR coefficients with the index combination $i,j=1,2$ or $k,l=1,2$. These terms are rather complicated and were not considered for the measurements. Each band is described by five parameters, the density n and the four mobility tensor elements μ_{11}, μ_{22}, μ_{33}, and μ_{12}. Primed and unprimed symbols are used to distinguish between the two bands. The types of the charge carriers are defined by the signs of e and e'. We introduce the following abbreviations:

$$\begin{aligned}
&\sigma_i=en\mu_{ii}+e'n'\mu'_{ii}\ ,\quad i=1,2,3\ ,\\
&\bar{\sigma}_{12}=en\mu_{12}+e'n'\mu'_{12}\ ,\\
&\Delta=\sigma_1\sigma_2-\bar{\sigma}_{12}^2\ ,\\
&\Delta_0=\sigma_3\Delta\ ,\\
&M=\mu_{11}\mu_{22}-\mu_{12}^2\ ,\\
&M'=\mu'_{11}\mu'_{22}-\mu'^2_{12}\ .
\end{aligned}\tag{A1}$$

The zero-field resistivities have the simple form

$$\rho_{11}=\frac{\sigma_2}{\Delta}\ ,\quad \rho_{22}=\frac{\sigma_1}{\Delta}\ ,\quad \rho_{33}=\frac{1}{\sigma_3}\ .\tag{A2}$$

For the Hall coefficients, we obtain

$$\rho_{213}=\frac{1}{\Delta}(enM+e'n'M')\ ,\tag{A3}$$

$$\rho_{132}=-\frac{1}{\Delta_0}[\bar{\sigma}_{12}(en\mu_{12}\mu_{33}+e'n'\mu'_{12}\mu'_{33})-\sigma_2(en\mu_{11}\mu_{33}+e'n'\mu'_{11}\mu'_{33})]\ ,\tag{A4}$$

$$\rho_{321}=-\frac{1}{\Delta_0}[\bar{\sigma}_{12}(en\mu_{12}\mu_{33}+e'n'\mu'_{12}\mu'_{33})-\sigma_1(en\mu_{22}\mu_{33}+e'n'\mu'_{22}\mu'_{33})]\ ,\tag{A5}$$

$$\rho_{131}=-\frac{1}{\Delta_0}[ene'n'(\mu'_{33}-\mu_{33})(\mu_{22}\mu'_{12}-\mu'_{22}\mu_{12})]\ ,\tag{A6}$$

$$\rho_{232}=-\frac{1}{\Delta_0}[ene'n'(\mu'_{33}-\mu_{33})(\mu_{11}\mu'_{12}-\mu'_{11}\mu_{12})]\ .\tag{A7}$$

The MR coefficients are given by

$$\rho_{3311}=\frac{1}{\sigma_3\Delta_0}\{ene'n'(\mu'_{33}-\mu_{33})^2[ne\mu'_{22}M+n'e'\mu_{22}M']\}\ ,\tag{A8}$$

$$\rho_{3322}=\frac{1}{\sigma_3\Delta_0}\{ene'n'(\mu'_{33}-\mu_{33})^2[ne\mu'_{11}M+n'e'\mu_{11}M']\}\ ,\tag{A9}$$

$$\rho_{3333}=0\ ,\tag{A10}$$

$$\rho_{2211}=\frac{1}{\Delta\Delta_0}\{ene'n'\mu_{33}\mu'_{33}[(\mu'_{22}-\mu_{22})\sigma_1-(\mu'_{12}-\mu_{12})\bar{\sigma}_{12}]\}^2\ ,\tag{A11}$$

$$\rho_{2222}=\frac{1}{\Delta\Delta_0}\{ene'n'\mu_{33}\mu'_{33}(ne+n'e')^2(\mu_{11}\mu'_{12}-\mu'_{11}\mu_{12})^2\}\ ,\tag{A12}$$

$$\rho_{2233}=\frac{1}{\Delta^2}\{ene'n'[neM'(\mu'_{11}\mu_{12}^2+\mu_{11}^2\mu'_{22}-2\mu_{12}\mu'_{12}\mu_{11})+enM(\mu'_{11}M-2\mu_{11}M')+e'n'M'(\mu_{11}M'-2\mu'_{11}M)+e'n'(\mu_{11}\mu'^2_{12}+\mu'^2_{11}\mu_{22}-2\mu'_{12}\mu_{12}\mu'_{11})]\}\ ,\tag{A13}$$

$$\rho_{3231}=\frac{1}{\Delta_0}ene'n'(\mu'_{33}-\mu_{33})(\mu_{12}M'-\mu'_{12}M)\ ,\tag{A14}$$

$$\rho_{3232}=\frac{1}{\Delta_0}ene'n'(\mu'_{33}-\mu_{33})(\mu'_{11}M-\mu_{11}M')\ ,\tag{A15}$$

$$\rho_{3131}=\frac{1}{\Delta_0}ene'n'(\mu'_{33}-\mu_{33})(\mu'_{22}M-\mu_{22}M')\ ,\tag{A16}$$

$$\rho_{3132}=\rho_{3231}\ .\tag{A17}$$

The MR coefficients with $i,j=1,1$ are obtained from Eqs. (A11)–(A13) by interchanging indices 1 and 2.

[1]W. Bauhofer, Phys. Rev. B **32**, 1183 (1985).
[2]W. Bauhofer, Phys. Rev. B **38**, 5215 (1988).
[3]R. v. Baltz, W. Denk, and W. Bauhofer, Phys. Rev. B **48**, 2098 (1993).
[4]B. L. Zhou, E. Gmelin, and W. Bauhofer, Solid State Commun. **51**, 757 (1984).
[5]A. C. Smith, J. F. Janak, and R. B. Adler, *Electronic Conduction in Solids* (McGraw-Hill, New York, 1967).
[6]*NAG Fortran Library Introductory Guide* (The Numerical Algorithms Group Limited, Oxford, 1991).